RSC Advances

PAPER

View Article Online
View Journal | View Issue

Cite this: *RSC Adv.*, 2020, **10**, 40157

An antibacterial and injectable calcium phosphate scaffold delivering human periodontal ligament stem cells for bone tissue engineering

Hong Chen,[abc] Hui Yang,[b] Michael D. Weir,[c] Abraham Schneider,[de] Ke Ren,[f] Negar Homayounfar,[c] Thomas W. Oates,[c] Ke Zhang,[*g] Jin Liu,[*ch] Tao Hu*[b] and Hockin H. K. Xu[cei]

Osteomyelitis and post-operative infections are major problems in orthopedic, dental and craniofacial surgeries. It is highly desirable for a tissue engineering construct to kill bacteria, while simultaneously delivering stem cells and enhancing cell function and tissue regeneration. The objectives of this study were to: (1) develop a novel injectable calcium phosphate cement (CPC) scaffold containing antibiotic ornidazole (ORZ) while encapsulating human periodontal ligament stem cells (hPDLSCs), and (2) investigate the inhibition efficacy against *Staphylococcus aureus* (*S. aureus*) and the promotion of hPDLSC function for osteogenesis for the first time. ORZ was incorporated into a CPC-chitosan scaffold. hPDLSCs were encapsulated in alginate microbeads (denoted hPDLSCbeads). The ORZ-loaded CPCC+hPDLSCbeads scaffold was fully injectable, and had a flexural strength of 3.50 ± 0.92 MPa and an elastic modulus of 1.30 ± 0.45 GPa, matching those of natural cancellous bone. With 6 days of sustained ORZ release, the CPCC+10ORZ (10% ORZ) scaffold had strong antibacterial effects on *S. aureus*, with an inhibition zone of 12.47 ± 1.01 mm. No colonies were observed in the CPCC+10ORZ group from 3 to 7 days. ORZ-containing scaffolds were biocompatible with hPDLSCs. CPCC+10ORZ+hPDLSCbeads scaffold with osteogenic medium had 2.4-fold increase in alkaline phosphatase (ALP) activity and bone mineral synthesis by hPDLSCs, as compared to the control group ($p < 0.05$). In conclusion, the novel antibacterial construct with stem cell delivery had injectability, good strength, strong antibacterial effects and biocompatibility, supporting osteogenic differentiation and bone mineral synthesis of hPDLSCs. The injectable and mechanically-strong CPCC+10ORZ+hPDLSCbeads construct has great potential for treating bone infections and promoting bone regeneration.

Received 10th August 2020
Accepted 26th October 2020

DOI: 10.1039/d0ra06873j

rsc.li/rsc-advances

1. Introduction

Osteomyelitis, is a common inflammatory and osteogenic response to an infecting microorganism that causes bone necrosis and destruction.[1,2] Despite advances in therapy, osteomyelitis remains notoriously difficult to treat and is responsible for significant morbidity.[3,4] In addition, post-operative infections are one of the main problems in orthopedic surgery as these infections often lead to failure of the surgical procedure, loss of bone tissue, and possible removal of implants requiring a second surgery.[5] The increase in systemic antibiotic usage and resistant pathogens has further complicated the management of osteomyelitis.[6]

Across all mechanisms leading to osteomyelitis, the occurrence of *Staphylococcus aureus* (*S. aureus*) is the predominant causative agent of worldwide.[4,7] In addition, methicillin-resistant *S. aureus* and vancomycin-resistant *S. aureus* has gradually increased.[6] Therefore, there is an acute need for developing tissue engineering constructs with local delivery of antibiotics. The normally-used systemic antibiotic doses may be

[a]*Department of Endodontics, College of Stomatological, Chongqing Medical University, Chongqing Key Laboratory of Oral Diseases and Biomedical Sciences, Chongqing Municipal Key Laboratory of Oral Biomedical Engineering of Higher Education, Chongqing, China*

[b]*State Key Laboratory of Oral Diseases, Department of Operative Dentistry and Endodontics, West China Hospital of Stomatology, National Clinical Research Centre for Oral Diseases, Sichuan University, Chengdu, China. E-mail: hutao@scu.edu.cn*

[c]*Department of Advanced Oral Sciences and Therapeutics, University of Maryland Dental School, Baltimore, MD 21201, USA. E-mail: liujin8511@163.com*

[d]*Department of Oncology and Diagnostic Sciences, University of Maryland School of Dentistry, Baltimore, USA*

[e]*Member, Marlene and Stewart Greenebaum Cancer Center, University of Maryland School of Medicine, Baltimore, MD 21201, USA*

[f]*Department of Neural and Pain Sciences, School of Dentistry, Program in Neuroscience, University of Maryland, Baltimore, MD 21201, USA*

[g]*Department of Orthodontics, School of Stomatology, Capital Medical University, Beijing, China. E-mail: tuzizhangke@163.com*

[h]*Key Laboratory of Shannxi Province for Craniofacial Precision Medicine Research, College of Stomatology, Xi'an Jiaotong University, Xi'an, Shannxi, China*

[i]*Center for Stem Cell Biology & Regenerative Medicine, University of Maryland School of Medicine, Baltimore, MD 21201, USA*

insufficient and yield inadequate therapeutic index and low bioavailability of the drug in local defects where it is needed.[8] In contrast, local delivery avoids the systemic antibiotic uses, thus reducing the potential development of antibiotic resistance.[9] Topical delivery of antibiotics is a novel therapeutic modality.[9] The local drug delivery systems can lead to high concentrations and long retention time of antibiotics in the administration site of infection, with no increase levels in the serum.[10] Drug-loaded poly-methyl methacrylate (PMMA) cements and drug-encapsulated PMMA beads were used for the localized delivery of antibiotics in infected bone defects.[10,11] However, PMMA-based materials produce polymerization heat with potential damage to local tissues, are non-resorbable, and require secondary surgical removal.[12]

Calcium phosphate cements (CPCs) are suitable for local drug delivery as they have multiple binding sites for loading various drugs.[5] Their delivery for drugs including antibiotics, anti-inflammatories, anti-cancer or anti-osteoporosis drugs was investigated.[13,14] In addition, CPCs have excellent injectability, osteoconductivity and osteoinductivity, and can be resorbable and replaced by new bone *in vivo*.[15,16] Therefore, CPCs are promising for treating infected bone defects in dental and craniofacial repairs.[14,17] One of these cements uses a powder with an equimolar mixture of tetracalcium phosphate [TTCP: Ca4(PO4)2O] and dicalcium phosphate-anhydrous [DCPA: CaHPO4], and is referred to as CPC.[16,17] The CPC paste is formed by mixing the powder with a liquid. The paste can be molded to the desired shape and then self-set and harden *in situ* to become a nanostructured and bone mineral-mimicking apatite scaffold in the bone defect.[14,17] Furthermore, incorporating chitosan into CPC could increase the strength and toughness of CPC, with non-cytotoxicity and supporting cell attachment and proliferation.[18,19] In addition, the antibacterial activity of chitosan itself is another advantage against bone infection.[20,21]

Ornidazole (ORZ) is a 5-nitroimidazole antibiotic drug widely used in treating anaerobic infections in periodontitis, endometritis, and anaerobic bone infections.[5,22] The antimicrobial activity of ORZ is based on the reduction of the nitro group to a more reactive amine group that attack microbial DNA, thus inhibiting the further synthesis.[23,24] Previous studies investigated ORZ delivery using biomaterials including CPCs and chitosan.[5,25,26] However, these previous studies did not investigate ORZ delivery in CPC-chitosan scaffold while encapsulating and delivering stem cells for bone tissue engineering. It is not clear whether the ORZ deliver, which could kill bacteria, would also harm the stem cells.

Combining biomaterial scaffold with seed cells can greatly enhance the tissue regeneration efficacy and functional recovery.[27,28] Human mesenchymal stem cells (hMSCs) have shown promise for tissue engineering and regenerative medicine.[29,30] Human periodontal ligament stem cells (hPDLSCs) are hMSCs isolated from the periodontal ligaments of extracted human teeth.[28,31,32] hPDLSCs can be harvested from teeth extracted for other purposes such as wisdom teeth and other teeth removed for orthodontic treatments, without an invasive procedure needed to harvest cells from the bone marrow. hPDLSCs possess high potential for dental, periodontal, maxillofacial and orthopaedic applications; however, there have been few reported studies on hPDLSCs. A few studies indicated that hPDLSCs differentiated into osteogenic cells,[31] cementoblasts,[33,34] chondrocytes,[33] fibroblasts[35] and adipocytes.[36] More effort is needed to investigate hPDLSCs for tissue engineering, especially when bacterial infection is present, such as in periodontal repair and regeneration.

Alginate is widely used in wound healing and tissue engineering due to its biocompatibility, low toxicity, relatively low cost, and mild gelation by addition of divalent cations such as Ca^{2+}.[37,38] In addition, alginate hydrogels retain structural similarity to the extracellular matrices in tissues and can provide a desirable environment for cell implantation.[37,38] Utilization of these gels enhances the rate of tissue regeneration by expediting disintegration of the hydrogel at the implantation site, thereby allowing for vascularization and subsequent tissue integration.[39,40] However, a literature search indicated that the use of alginate microbeads combined with hPDLSCs in tissue engineering has not been reported. To date, there has been no report on the development of an injectable CPC-chitosan scaffold containing alginate microbeads with local delivery of ORZ and hPDLSCs.

Therefore, the objectives of this study were to: (1) develop a novel injectable CPC-chitosan scaffold containing alginate microbeads with antibacterial and bone tissue engineering capabilities; and (2) investigate the effects on *S. aureus* biofilm inhibition, as well as hPDLSC proliferation, osteogenic differentiation and bone mineral synthesis for the first time. Three hypotheses were tested: (1) the ORZ-loaded CPC-chitosan-alginate microbead scaffold would have good injectability and mechanical strength; (2) the construct would have a sustained ORZ release and a strong killing efficacy against *S. aureus*; and (3) the construct could encapsulate and deliver hPDLSCs with enhanced cell proliferation and osteogenesis.

2. Materials and methods

2.1. hPDLSCs culture and seeding

Periodontal ligament (PDL) tissues were obtained with informed consent from human adult premolars that were extracted for orthodontic purposes.[31,32] All experiments were performed in accordance with the guidelines of the National Institutes of Health (NIH), and the procedures were approved by the Institutional Review Board of the authors' university (approval ID: HP-00079029). The hPDLSCs were isolated and characterized as described in previous studies.[41,42] At 80–90% confluence, hPDLSCs were detached and passaged, and passage 3–5 cells were used.[41,42] The culture medium was a low-glucose Dulbecco's modified Eagle's medium (DMEM, Gibco, Grand Island, NY, USA) supplemented with 10% fetal bovine serum (FBS) and 1% penicillin-streptomycin (Invitrogen, Carlsbad, CA) (control media).[41,42] The cells were incubated at 37 °C with 5% CO_2 and the culture medium was changed at every 2–3 days. The osteogenic medium consisted of the DMEM supplemented with 10% FBS, 1% penicillin/streptomycin, 100 nM dexamethasone, 10 mM β-glycerophosphate, 0.05 mM ascorbic acid, and 10 nM 1α,25-dihydroxyvitamin (Millipore).[41,42] In our previous study,[32]

immunofluorescence staining showed that STRO-1 was positive and the CD34 was negative in the hPDLSCs. The molecular surface antigen markers in hPDLSCs by flow cytometry indicated that the cells were positive for STRO-1, CD146 and OCT4, weakly negative for Nanog and negative for CD34 and CD45. The hPDLSCs also had the ability to different into osteogenic, fibrogenic and cementogenic lineages, suitable for regeneration of the periodontal complex.[32]

2.2. Preparation of CPC-chitosan scaffold samples

TTCP was synthesized from a solid–state reaction of DCPA and calcium carbonate (J. T. Baker, Phillipsburg, NJ), which were mixed and heated at 1500 °C for 6 hours in a furnace (Model 51333, Lindberg, Watertown, WI, USA).[43,44] The heated mixture was quenched to room temperature, then ground in a ball mill (Retsch PM4, Brinkman, NY, USA) and sieved to obtain TTCP particles with a median particle size of 5 μm. DCPA powder was ground for 24 hours in the ball mill in 95% ethanol and sieved to obtain a median particle size of approximately 1 μm. TTCP and DCPA powders were mixed in a blender at a molar ratio of 1 : 1 to form the CPC powder.[30,44,45]Antibiotic ORZ (Sigma Aldrich, St. Louis, MO, USA) was added to CPC powder at 5% and 10% mass fractions, respectively, and mixed using a mortar and pestle.[5]

Chitosan lactate (Halosource, Redmond, WA, USA), referred to as chitosan, was modified with covalently conjugated G4RGDSP oligopeptides (Peptides International, Louisville, KY, USA) using carbodiimide chemistry.[45,46] Chitosan was dissolved in de-ionized water (DI water) at a mass fraction of 7.5% following a previous study.[44] This liquid was mixed with CPC power at a mass ratio of 2 : 1 following a previous study.[47,48] The addition of chitosan was to make the CPC paste to have a faster setting time and higher mechanical strength.[49]

To deliver stem cells for tissue engineering, the direct mixing of cells into CPC paste would kill the cells due to the mechanical mixing forces and the setting reaction. Therefore, cells were first encapsulated into alginate hydrogel microbeads, and then these microbeads were mixed with CPC paste. The microbeads would protect the cells from the mixing forces. Once the CPC has set, the microbeads were degraded to release the cells throughout the CPC-chitosan scaffold volume. A 1.2% (by mass) sodium alginate solution was prepared by dissolving alginate (UP LVG, 64% guluronic acid, MW = 75 000–220 000 g mol^{-1}, ProNova, Oslo, Norway) in a saline solution at 37 °C (155 mmol L^{-1} NaCl), following previous studies.[19,28,41] hPDLSCs were added to the alginate solution at a density of 1×10^6 cells per mL.[28,41] The alginate solution were loaded into a syringe which was placed into a syringe pump and connected to a bead-generating device (Var J1, Nisco, Zurich, Switzerland) for microbeads formation.[28,41] Nitrogen gas was fed to the gas inlet and a pressure of 10 psi was applied to break up the alginate droplets.[28,41] The droplets fell into a well of 0.1 mol L^{-1} calcium chloride solution and crosslinked to form microbeads (hPDLSC-encapsulating-microbeads).[30] A microbead volume fraction of 50% was incorporated into CPC-chitosan paste (CPCC+hPDLSCbeads). This could encapsulate a relatively large amount of cells, and then create 50% macropore volume fraction in CPC-chitosan scaffold after microbead dissolution.[30]

Three groups were tested for mechanical properties and injectability:

(1) CPC-chitosan scaffold control (CPCC control);

(2) 5% ORZ-loaded CPC-chitosan containing alginate microbeads encapsulating hPDLSCs (CPCC+5ORZ+hPDLSCbeads);

(3) 10% ORZ-loaded CPC-chitosan containing alginate microbeads encapsulating hPDLSCs (CPCC+10ORZ+hPDLSCbeads).

2.3. Mechanical testing

Mechanical properties were evaluated using three-point flexure to measure flexural strength, elastic modulus and work-of-fracture (WOF). Three groups were tested and six specimens were prepared per group ($n = 6$). Each paste was placed into molds of 3 × 4 × 25 mm. The specimens were incubated in a humidor for 4 h at 37 °C. The hardened specimens were demolded and immersed in the culture medium for 1 day. A three-point flexural test was used to fracture the specimens on a computer-controlled Universal Testing Machine (MTS, Eden Prairie, MN, USA). Flexural strength $S = 3F_{max}L/(2bh^2)$, Where Fmax is the maximum load on the load-displacement (F–d) curve, L is the span, b is the specimen width and h is the thickness.[50] Elastic modulus $E = (F/d)\,(L^3/[4bh^3])$,[51] where load F divided by displacement d is the slope. WOF was calculated as the area under the F–d curve divided by the sample's cross-sectional area.[18,43]

2.4. Injectability

To measure the injectability of the CPC-chitosan scaffolds, a 10 mL syringe (Free-Flo, Kerr, Romulus, MI, USA) was used with a tip opening of 2.7 mm, following a previous study.[30] The CPC-chitosan pastes were mixed and filled into the syringe which was pressed *via* the Universal Testing Machine.[30] The compression was started and the paste was extruded until the paste was entirely extruded.[30,48] The percentages of paste extruded were compared to the original mass in the syringe ($n = 6$).[30,48] The injection force was recorded and the maximum force was used as the injection force ($n = 6$).[30,48]

2.5. Drug release from CPC-chitosan paste *in vitro*

The ORZ-loaded CPC-chitosan samples were prepared using a disk mold with 10 mm in diameter and 0.8 mm in thickness. The weight of the samples was kept constant at 150 mg. After incubation at 37 °C in a humidor for 1 day, each specimen was immersed in 40 mL phosphate buffered saline (PBS) pH 7.4 at 37 °C.[52,53] The rate of drug release from the cements was tested by collecting 1 mL of PBS after 0, 0.5, 1, 2, 3, 4, 14, 24 hours, and then once every day until day 7. The retrieved solution was replenished each time with fresh PBS. A 96-well plate was used and the OD318 nm was determined using a microplate reader (SpectraMax M5, Molecular Devices, Sunnyvale, CA, USA) ($n = 6$).[53,54] Seven standard ORZ concentrations of 0, 3.91, 7.82, 15.63, 31.25, 62.5, 125 and 250 mg L^{-1} were used to plot the standard curve, and the standard curve was used to calculate the drug release concentration.

2.6. Bacterial culture

The use of *S. aureus* strain ATCC29213 was approved by the Institutional Review Board of the University of Maryland Baltimore. The *S. aureus* were cultured in Tryptic Soy Broth (TSB) (Sigma, St. Louis, MO, USA), and incubated at 37 °C with 5% CO_2.[54] Three CPC-chitosan scaffolds were used with molds having a diameter of 10 mm and a thickness of 1 mm. Sterilized CPCC control, CPCC+5ORZ, and CPCC+10ORZ were tested for antibacterial properties. The CPC-chitosan disks were sterilized in an ethylene oxide sterilizer (Andersen, Haw River, NC, USA) for 24 hours and then degassed for 7 days.[31] For biofilm formation, each sterilized CPC-chitosan scaffold disk was placed into a well of 24-well plates. The overnight bacterial suspension was diluted by fresh TSB medium supplemented with 0.5% glucose (TSB-G) to 10^7 colony-forming units (CFU) mL^{-1}.[55] The bacteria concentrations of the inoculum were determined using a spectrophotometer (Genesys 10S, Thermo Scientific, Waltham, MA, USA). The cultures were incubated at 37 °C with 5% CO_2 for 7 days to grow biofilms on CPC-chitosan scaffold disks.

2.7. Agar disk-diffusion test

Agar disk diffusion test (ADT) was used to examine the antibacterial effect of CPC-chitosan scaffolds.[56,57] Three CPC-chitosan groups were tested with molds having a diameter of 10 mm and a thickness of 1 mm. Four groups were tested: blank paper, CPCC control, CPCC+5ORZ, and CPCC+10ORZ. The plates containing 20 mL of tryptic soy agar (TSA) (Sigma) were used, and 100 μL of bacterial suspensions (10^6 CFU mL^{-1}) were spread thoroughly all over the surface of TSA.[56] All the groups were placed in the center of *S. aureus* TSA plates. The agar plates were incubated at 37 °C in 5% CO_2 for 7 days.[57] Bacteria inhibition zone size = (outer diameter of inhibition zone − paper disk diameter)/2.[58]

2.8. Biofilm CFU counts

To measure biofilm CFU counts, three CPC-chitosan groups were used with a diameter of 10 mm and a thickness of 1 mm: (1) CPCC control; (2) CPCC+5ORZ; (3) CPCC+10ORZ. Six disks of each group were used ($n = 6$). Then the sterilized CPC-chitosan scaffold disks were placed into 24-well plates. Each well of a 24-well plate was inoculated with exponential cultures of bacteria and TSB-G at a concentration of 10^7 CFU mL^{-1}.[55] The cultures were incubated at 37 °C with 5% CO_2 for 1, 3, 5, and 7 days.[59] After incubation, the medium was gently removed and the biofilms were washed three times with PBS. The biofilms were harvested in PBS by scraping and sonication/vortexing (Fisher, Pittsburg, PA, USA). The bacterial suspensions were serially diluted and spread on TSA plates.[60] After 24 hour incubation at 37 °C in 5% CO_2, the colony number was counted and the CFU counts were determined.[59]

2.9. Live/dead bacteria assay of biofilms

Three CPC-chitosan groups were used: (1) CPCC control; (2) CPCC+5ORZ; (3) CPCC+10ORZ. Six samples for each group with 1 day biofilms were washed with PBS, then stained with BacLight Live/Dead bacterial viability kits (Molecular Probes, Eugene, OR, USA) ($n = 6$).[61] A mixture of 2.5 μM SYTO 9 and 2.5 μM propidium iodide was set on each sample for 15 min. The live bacteria were stained by SYTO 9 to a green color, and the compromised bacteria were stained by propidium iodide into a red color. Images were captured with an inverted epifluorescence microscope (TE2000-S, Nikon, Melville, NY, USA). Six disks were used for each group and each disk was tested in five random positions, yielding 30 images per group.

2.10. Cytotoxicity testing using hPDLSCs

The hPDLSCs were used to examine the cytotoxicity of three groups: (1) CPCC control; (2) CPCC+5ORZ; (3) CPCC+10ORZ. The sterilized disks for the three groups were placed in a 24-well plate, immersed in PBS for 1 hour, and then incubated in DMEM (Gibco, Invitrogen, USA) containing 10% FBS and 1% penicillin/streptomycin. The extract of DMEM medium from the cement samples was retrieved after 24 hours and methyl thiazolyl diphenyltetrazolium bromide (MTT, VWR Chemicals, Ohio, USA) assay was performed.[5] The hPDLSCs were seeded at a cell density of 50 000 cells per well in DMEM medium. After 24 hours, when the cells achieved about 50% confluency, DMEM present in the well plate was replaced with the extract collected from the cement samples. After 24, 48 and 72 hours, the extracts were replaced with growth medium containing 0.5 mg mL^{-1} MTT and incubated for 1 hour. Dimethyl sulfoxi (DMSO) was added to each well and incubated for 20 min to dissolve the formazan crystals. The DMSO solution was then transferred into 96-well plate and OD_{540nm} was determined using a microplate reader (SpectraMax M5, Molecular Devices).[59]

The hPDLSCs cultured with DMEM (Gibco) containing 10% FCS (Gibco) and 1% penicillin/streptomycin (Invitrogen) were used as the negative control. The percentage cell viability was assessed using cell viability = OD of the CPC-chitosan scaffolds/OD of the negative control group.[5]

2.11. Live/dead staining for cells

CPCC+5ORZ and CPCC+10ORZ groups had cell viability > 90%. In addition, CPCC+10ORZ had a sustained drug release for a longer time and had a better antimicrobial activity, compared to CPCC+5ORZ. Therefore, CPCC+10ORZ was selected to test with hPDLSC-encapsulating alginate microbeads. 50% by volume of hPDLSC-encapsulating alginate microbeads were added on CPCC+10ORZ scaffold disks.

Three groups were tested:

(1) Control group (CPCC+hPDLSCbeads, cultured in control medium);

(2) Osteogenic group (CPCC+hPDLSCbeads, cultured in osteogenic medium);

(3) ORZ+osteogenic group (CPCC+10ORZ+hPDLSCbeads, cultured in osteogenic medium).

The live/dead viability kit (Molecular Probes, Eugene, OR, USA) was used to investigate the cell viability in alginate beads in CPC-chitosan for stem cell encapsulation. Each sterilized disk and 50% by volume of hPDLSC-encapsulating alginate

microbeads was placed into a well of 24-well plates, and control medium or osteogenic medium was added. The plates were incubated at 37 °C with 5% CO_2 and the culture medium was changed every 1–2 day. After culturing for 1, 4, 7, and 14 days, the medium was removed, and the microbeads and cells around the disks were washed twice with PBS. Before staining, the hPDLSCs and hPDLSC-encapsulating microbeads around the scaffolds were viewed *via* an epifluorescence microscopy (Eclipse TE2000-S, Nikon, Melville, NY, USA). Then, CPC-chitosan disks were incubated with 4 mM ethidium homodimer-1 (EthD-1) and 2 mM calcein-AM in PBS for 20 minutes. Three randomly chosen fields of view were captured for each specimen. Six specimens ($n = 6$) yielded 18 images for each time point for each group. The live (green) and dead (red) cells were counted. The live cell density (D) and the percentage of live cells (P) were calculated. D = number of live cells in the image/the image area.[31] P = number of live cells/(number of live cells + number of dead cells).[31]

2.12. CCK-8 for cells

Three groups were tested for cell proliferation: (1) control group; (2) osteogenic group; (3) ORZ+osteogenic group. Each sterilized disk and 50% by volume of hPDLSC-encapsulating alginate microbeads was placed into a well of 24-well plates. Control medium or osteogenic medium was added accordingly, and changed every 2–3 day. A cell counting kit (CCK-8, Dojindo, Tokyo, Japan) was used to evaluate cell proliferation. Six replicates in each group were used for this assay ($n = 6$). After 1, 4, 7, and 14 days, the disks were washed twice with PBS, and gently removed to a new 24-well plate. 300 μL of growth medium with 10% CCK-8 for 2 hours added into each well, and the cell proliferative rate was determined *via* measuring the absorbance at OD450 nm using a microplate reader (SpectraMax M5, Molecular Devices).[31]

2.13. ALP staining and ALP activity assay

Three groups were tested for ALP staining and ALP activity assay: (1) control group; (2) osteogenic group; (3) ORZ+osteogenic group. Each sterilized disk and 50% by volume of hPDLSC-encapsulating alginate microbeads was placed into a well of 24-well plates. Control medium or osteogenic medium was added accordingly, and changed every 2–3 day. After incubation for 14 days, the cells were stained with ALP Staining Kit (Red) (abcom, ab242286). Before staining, the disks were washed twice with PBS, and gently removed to a new 24-well plate. Then the disks and cells were fixed with the fixing solutions for 2 min, and stained with an ALP staining kit for 20 min.[32]

At 14 days, the hPDLSCs on disks' surface were washed by PBS, and then removed to a new 24-well plate. 0.2% Triton X-100

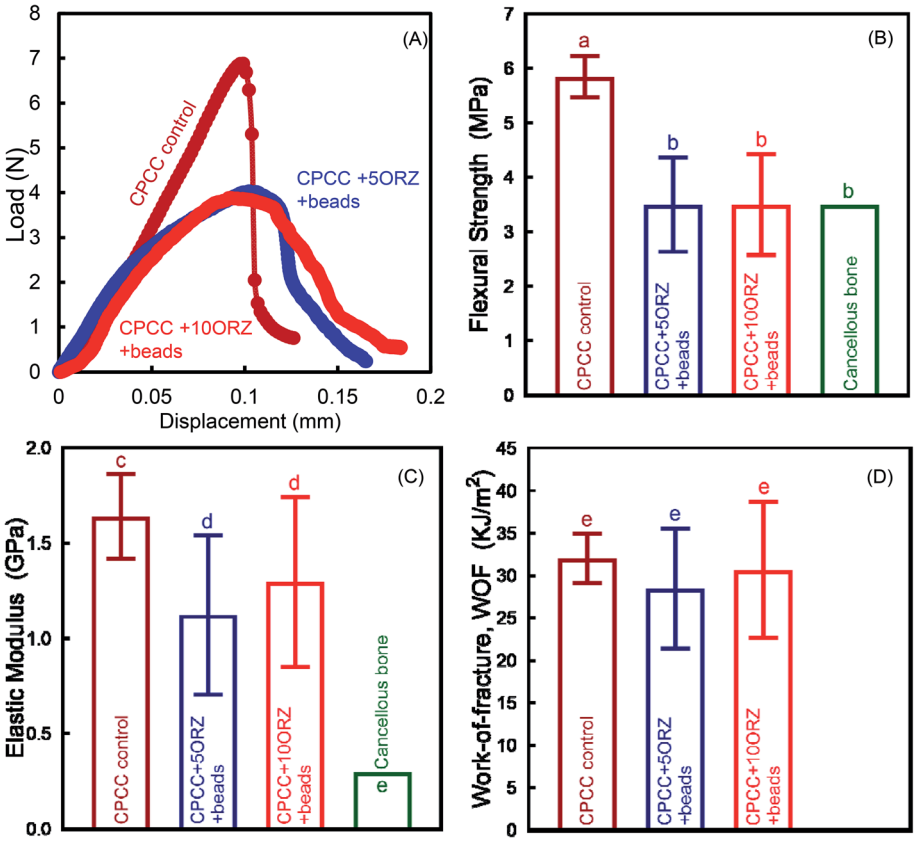

Fig. 1 Mechanical properties of CPC-chitosan scaffolds (mean ± sd; $n = 6$). Typical load–displacement curves (A); Flexural strength (B), elastic modulus (GPa) (C), and work-of-fracture (D). Values with dissimilar letters are significantly different from each other ($p < 0.05$).

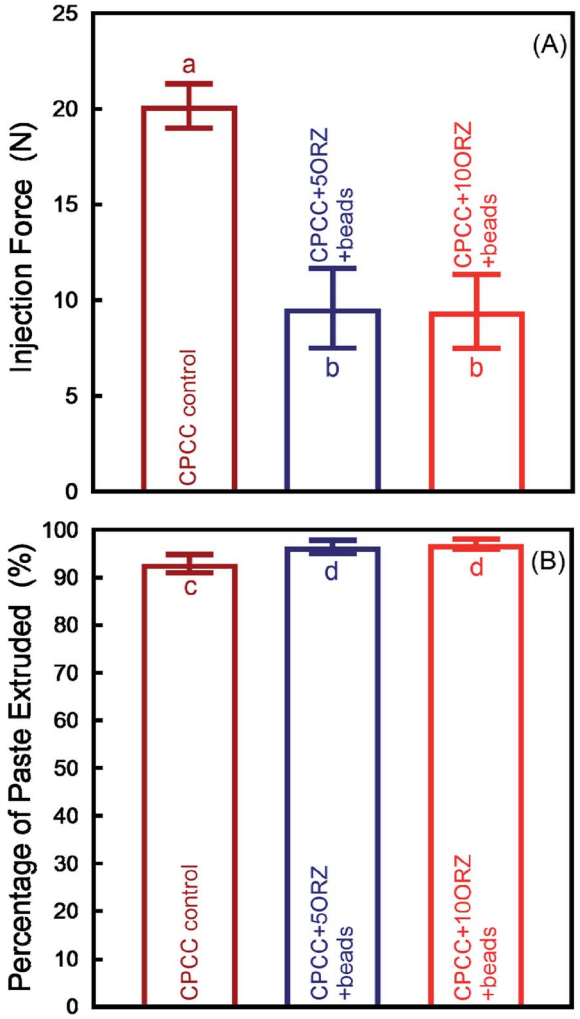

Fig. 2 Injectability of the CPC-chitosan scaffolds (mean ± sd; $n = 6$). Injection force (A), and percentage of paste extruded (B). Dissimilar letters indicate significantly different values ($p < 0.05$).

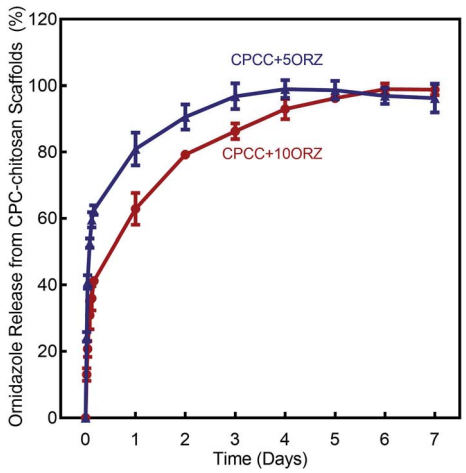

Fig. 3 The drug release profile of ornidazole (ORZ) from CPC-chitosan scaffolds (mean ± sd; $n = 6$). After an initial burst of release of nearly 50% of the dose in 12 hour, the complete ORZ release was observed in the 3rd and 6th day for CPCC+5ORZ and CPCC+10ORZ, respectively.

(Millipore Sigma) solution was used to lyse the hPDLSCs on disks.[31,32] An alkaline phosphatase assay kit (QuantiChrom, BioAssay Systems, Hayward, CA, USA) with *p*-nitrophenylphosphate (pNPP) as a substrate was used to measure the ALP activity of the cell lysate.[31,32] The ALP activity was determined by measuring the absorbance at an optical density of 405 nm using a microplate reader (SpectraMax M5).[31] The protein of cell lysate was quantified using a protein assay kit (Pierce BCA, Thermo Scientific, Rockford, IL, USA) following the manufacturer's protocol. The ALP activity was normalized to the protein amount and reported as U/g protein.[31]

2.14. Mineral synthesis by the hPDLSCs

Four groups were tested for the mineral synthesis by hPDLSCs: (1) non-hPDLSCs group: CPC-chitosan-alginate microbead scaffolds without hPDLSCs; (2) control group; (3) osteogenic group; (4) ORZ+osteogenic group. Each sterilized disk and 50% by volume of hPDLSC-encapsulating alginate microbeads was placed into a well of 24-well plates. Control medium or

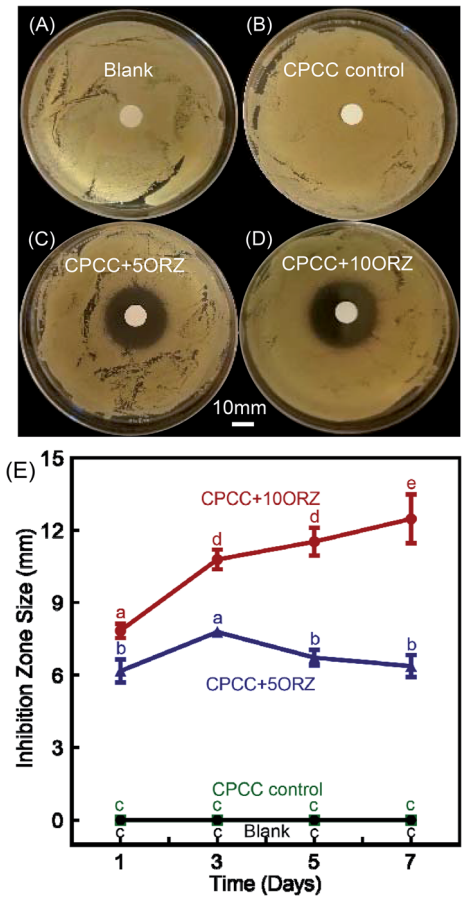

Fig. 4 Antimicrobial activity of CPC-chitosan scaffolds against *S. aureus* biofilm. The 24 hour images of the samples against *S. aureus* (A–D). The bacteriostatic rings of CPC-chitosan scaffolds against *S. aureus* (E) (mean ± sd; $n = 6$). Dissimilar letters indicate significantly different values ($p < 0.05$).

osteogenic medium was added accordingly, and changed every 2–3 day. At 14 days, the hPDLSCs on scaffolds were washed by PBS, and then removed to a new 24-well plate. Then the hPDLSCs were fixed with 10% formaldehyde for 45 minutes and stained with Alizarin Red S (ARS, Millipore, Billerica, MA, USA) for 30 minutes ($n = 6$).[31] The ARS stained the mineral deposits synthesized by the cells into a red color. After staining, the ARS solution was removed, and the disks were washed gently with PBS to remove any loose ARS.[31] Then the specimens were imaged. For quantification, the stained disks were desorbed using 10% cetylpyridinium chloride (Millipore) for 1 hour and the concentration was measured at optical density of 550 nm using a microplate reader (SpectraMax M5).[62] Blank CPCC scaffolds with the same treatments, but without cell seeding, were also measured.[31] The value of blank CPCC scaffolds was subtracted from the value of the cell-seeded scaffolds to calculate the mineral concentration synthesized by the cells.[31]

2.15. Statistical analysis

Data analyses were conducted using a statistical software SPSS 19.0 (SPSS, Chicago, IL, USA). All data were expressed as the mean value ± standard deviation (SD). One-way or two-way analyses of variance (ANOVA) were tested to detect the significant effects of the variables. Tukey's multiple comparison tests were performed. The significance level of p was set at 0.05.

3. Results

Fig. 1 shows the effect of incorporation of alginate microbeads and ORZ on the mechanical properties of CPC-chitosan scaffold. Typical load–displacement curves are shown in Fig. 1A. The addition of alginate microbeads reduced the load-bearing capability and increased the flexibility and displacement to failure, likely due to the additional water content from the alginate microbeads. The CPCC+hPDLSCbeads construct

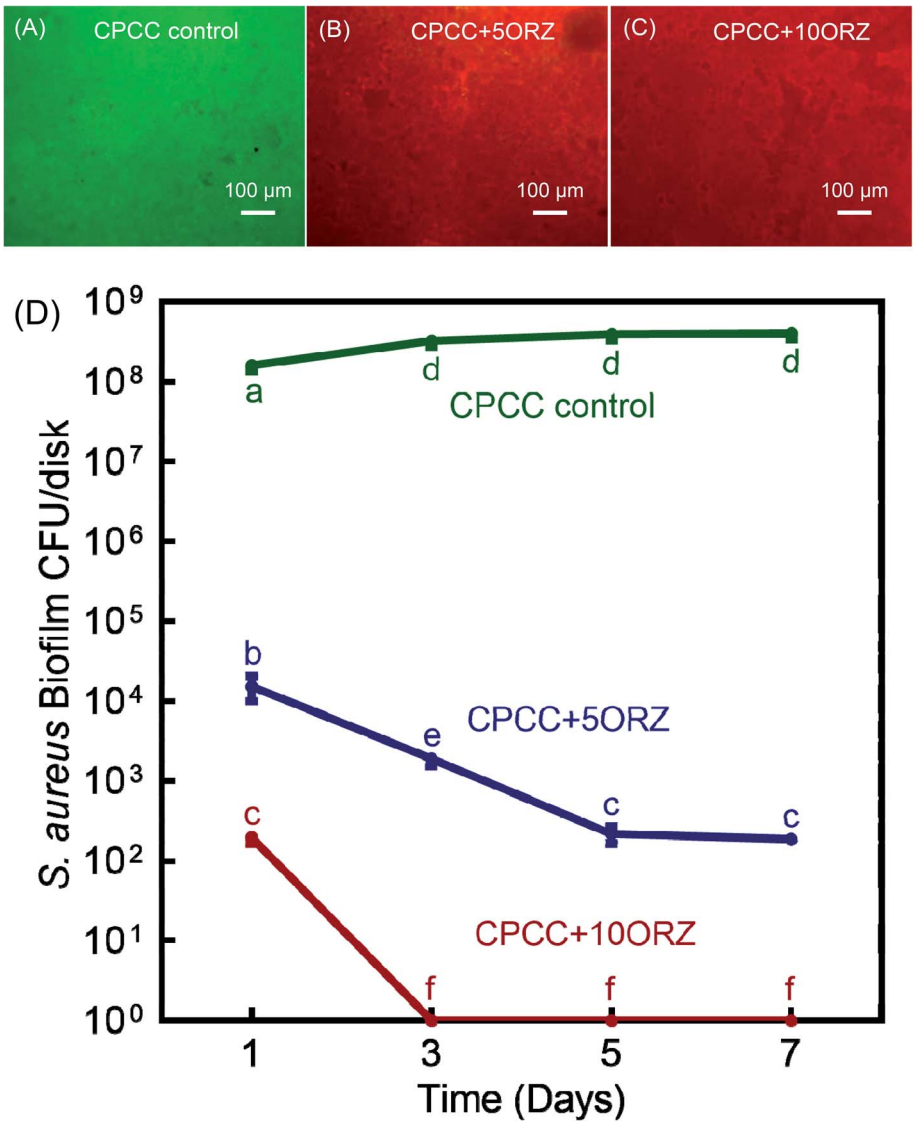

Fig. 5 Representative live/dead staining images of 24 hour *S. aureus* biofilms (A–C). Time-kill curve showing log reduction against *S. aureus* (D) (mean ± sd; $n = 6$). Dissimilar letters indicate significantly different values ($p < 0.05$).

exhibited a slight decrease in flexural strength when compared to CPCC control (Fig. 1B) ($p < 0.05$). However, the flexural strength of CPCC+hPDLSCbeads matched that of natural cancellous bone (Fig. 1B). The elastic moduli are plotted in Fig. 1C. With increasing the mass fraction of ORZ from 5% to 10%, the flexural strength and elastic modulus showed no significant decrease ($p > 0.05$). There was no significant difference in WOF among the groups (Fig. 1D). As shown in Fig. 2A, CPCC+hPDLSCbeads had a lower injection force, compared to CPCC control ($p < 0.05$). The percentages of extruded paste for CPCC+hPDLSCbeads were significantly increased when compared to CPCC control (Fig. 2B) ($p < 0.05$). These results demonstrate that adding ORZ into CPC did not negatively affect the mechanical properties and the injectability, and the injectable CPCC+hPDLSCbeads had a strength matching that of cancellous bone.

The ORZ release from scaffolds is shown in Fig. 3. After an initial burst release of nearly 50% of the dose in 12 hour, 100% drug release was observed on the 3rd and 6th day for CPCC+5ORZ and CPCC+10ORZ, respectively. CPCC+10ORZ showed a release longer time than CPCC+5ORZ.

The ADT results are shown in Fig. 4. One day results of the samples with and without ORZ against *S. aureus* are shown in Fig. 4A–D. The inhibition zone in the samples without ORZ was similar to the blank control, and both of them showed no antimicrobial activity ($p > 0.05$). CPCC+5ORZ and CPCC+10ORZ exhibited strong antimicrobial activity against *S. aureus.* The inhibition zone sizes of CPCC+5ORZ and CPCC+10ORZ were more than 6 mm at 1 day (Fig. 4E). The inhibition zone sizes of CPCC+10ORZ increased from 1 to 7 days.

Representative live/dead images of 1 day *S. aureus* biofilms are shown in Fig. 5A–C. Fig. 5D recorded the biofilm CFU counts for 1, 3, 5 and 7 days. No colonies were observed in CPCC+10ORZ group from 3 days to 7 days. These results demonstrate that adding ORZ at 5% and 10% mass fractions in CPC-chitosan scaffolds could significantly increase the anti-microbial activity. The CPCC+10ORZ construct had an excellent and stable bacterial killing efficacy.

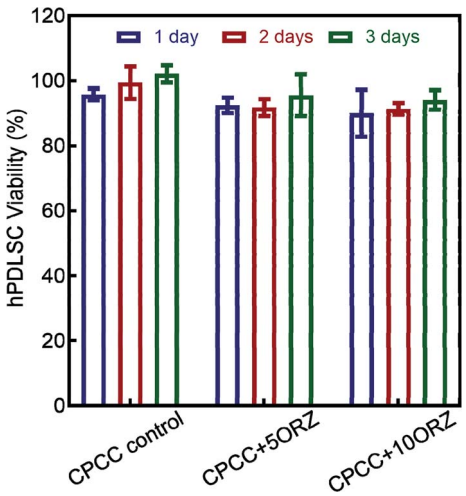

Fig. 6 Cell viability assay of CPC-chitosan scaffolds with and without ornidazole (ORZ) addition (mean ± sd; $n = 6$). CPCC+5ORZ and CPCC+10ORZ groups had cell viability of above 90%. An increasing trend of the hPDLSC viability was shown in all groups over time.

The viability of hPDLSCs seeded on CPC-chitosan scaffolds is shown in Fig. 6. All groups had cell viability of above 90%. However, ORZ-containing samples showed a slight decrease in cell viability. With increasing time, an increasing trend of the hPDLSCs viability was shown in all groups. These results show that CPCC+5ORZ and CPCC+10ORZ had good biocompatibility. Due to the strong and stable anti-microbial activity, CPCC+10ORZ+beads scaffold was selected to test the delivery of hPDLSCs and differentiation into the osteogenic lineage.

Fig. 7 compared the viability of the encapsulated hPDLSCs. The hPDLSCs inside the alginate microbeads was not adversely affected by the paste mixing and injection forces, as shown by the live/dead staining in Fig. 7K–O. Live cells appeared as green dots dispersed in microbeads, with a few dead cells (Fig. 7K–O). At 4 days, some cells were released from the microbeads due to alginate hydrogel degradation, which was beneficial because the delivered and released cells could proliferate and differentiate into the osteogenic lineage. The released cells exhibited a healthy spreading and polygonal morphology (Fig. 7C, H and M). From 7 to 14 days, as more cells were released, cell proliferation was significantly enhanced.

Fig. 8A–L show representative live/dead images at 1, 4, 7 and 14 days. Live cells (stained green) had spreading and were numerous in all three groups. Dead cells (stained red) were relatively few. This indicates that the hPDLSCs exhibited good compatibility and good viability on CPC-chitosan scaffolds. Fig. 8M shows that the percentages of live cells on CPC-chitosan scaffolds in all three groups were about 95%. At 14 days, no significant difference was found between the three groups ($p > 0.05$). In Fig. 8N, the results of CCK-8 showed that the cell proliferation was significantly increased from 1 to 14 days. No significant difference was found between three groups ($p < 0.05$). These results demonstrate that the viability of hPDLSCs encapsulated inside the alginate microbeads was not adversely affected by the paste mixing and injection process. Furthermore, at 14 days, the microbeads were completely degraded to release the cells throughout the CPC-chitosan scaffold volume. The attachment and spreading of the cells demonstrated the biocompatibility of the scaffolds.

The osteogenic differentiation of hPDLSCs in CPC-chitosan scaffolds was evaluated by measuring ALP activity and staining of the calcium marker Alizarin Red at 14 days (Fig. 9). The ALP activity results show that the control group was the lowest among the three groups ($p < 0.05$). The ALP activity of the osteogenic group was more than 2.5 folds higher than that of control ($p < 0.05$; Fig. 9A). The ALP activity of ORZ+osteogenic was more than 2 folds higher than that of the control group ($p < 0.05$; Fig. 9A). In Fig. 9B, at 14 days, the ARS staining was deeper and denser for osteogenic group and ORZ+osteogenic group than for control group and non-hPDLSCs group. More calcium nodules were formed by hPDLSCs in the osteogenic group and ORZ+osteogenic group than the control group ($p < 0.05$). These results demonstrate that the hPDLSCs released from the

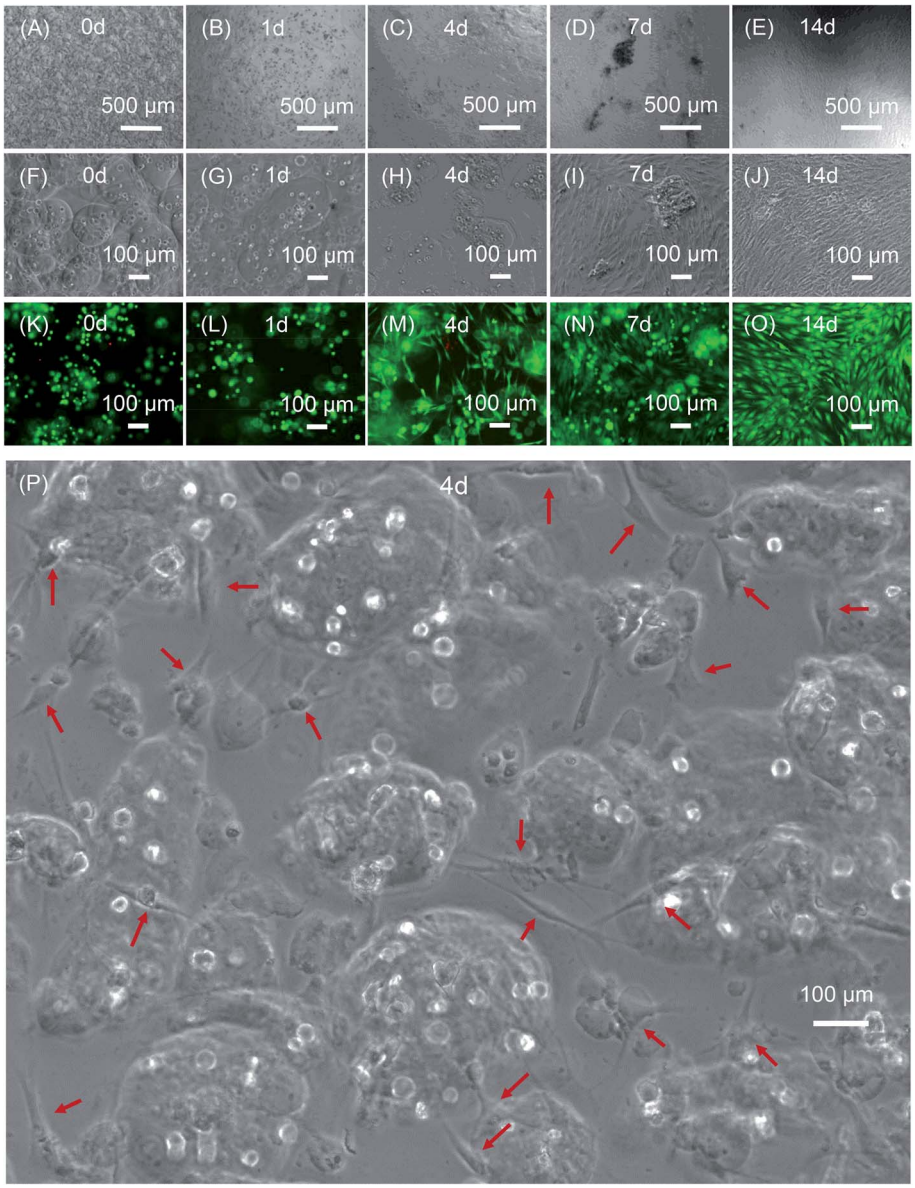

Fig. 7 Cell encapsulation and release from alginate microbeads (without the CPC-chitosan scaffolds) at 0 day (A, F and K). To examine microbeads degradation and cell release, 50% by volume of hPDLSC-encapsulating alginate microbeads was placed on the sterilized CPC disks. At 1 day, cell-encapsulating microbeads were collected and imaged (B, G and L). In the culture medium, the microbeads gradually degraded and the hPDLSCs (red arrows) started to be released from the microbeads at 4 days (C, H, M and P). More cells were released, and the contour of the microbeads became obscure as the alginate degraded from 4 to 14 days (D, E, I, J, N and O).

microbeads were differentiated into the osteogenic lineage and synthesized bone minerals.

4. Discussion

The present study developed a novel injectable ORZ-loaded CPC-chitosan scaffold with hPDLSCs in alginate microbeads, showing the ability to inhibit *S. aureus* infection while simultaneously promoting osteogenic differentiation of hPDLSCs for bone regeneration. The hypotheses were proven that the novel injectable 10% ORZ-loaded CPC-chitosan construct exhibited an excellent injectability, good mechanical strength, and a potent killing efficacy against *S. aureus*. ORZ release from the drug-loaded CPC-chitosan scaffold slightly reduced the cell viability.[5] However, a healthy proliferation of the cells continued, indicating the biocompatible nature of the scaffold. In addition, the released hPDLSCs on the CPC scaffold were able to attach to the scaffold, differentiated into the osteogenic lineage, and synthesized bone minerals *in vitro*. Therefore, the novel injectable CPCC+10ORZ+hPDLSCbeads construct is promising for bone tissue engineering applications.

One disadvantage of injectable hydrogel is the weak mechanical properties, making them incapable to withstand pressure or to maintain the shape integrity.[30,63] In the present

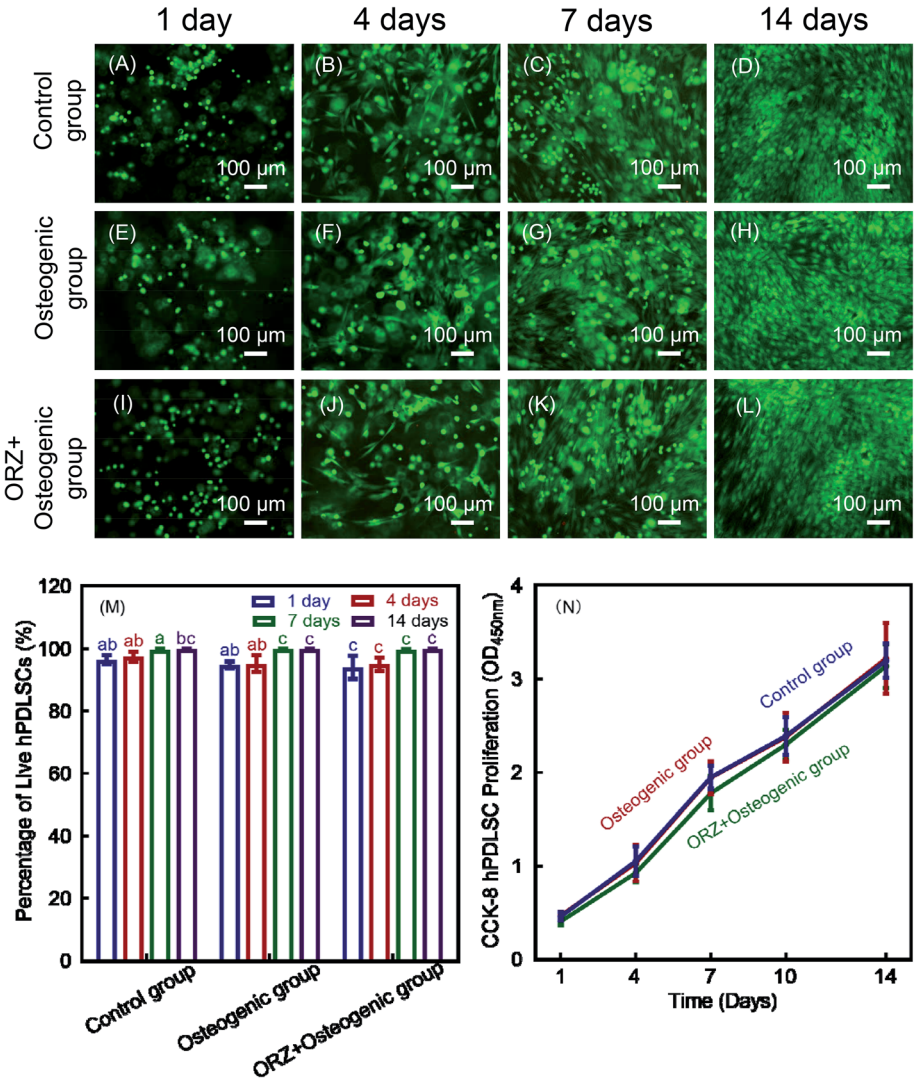

Fig. 8 Live/dead images of hPDLSCs encapsulated in alginate microbeads in CPC-chitosan scaffolds (A–L). Live cells (green) were numerous and dead cells (red) were very few. Percentages of live cells (M) and CCK-8 from 1 to 14 days showed good cell viability and proliferation, and cell viability, which was not negatively affected by injection force and the delivery of ORZ (N) (mean ± sd; $n = 6$). Dissimilar letters indicate significantly different values ($p < 0.05$).

study, the novel injectable CPCC+10ORZ+hPDLSCbeads had load-bearing capability after injection and CPC setting. The novel scaffold had a flexural strength of 3.50 MPa and an elastic modulus of 1.30 GPa, which matched the reported strength of natural cancellous bone.[64] After CPC-chitosan scaffold setting, with rapid degradation of the alginate microbeads, the cells could be released to attach to the macropores in the CPC-chitosan scaffold.[63] The CPC-chitosan scaffold provided a biocompatible substrate for cell attachment, proliferation and differentiation. In addition, the scaffold demonstrated excellent injectability, and the paste is suitable for filling irregularly-shaped bone defects.[65,66] Furthermore, unlike the exothermic setting of PMMA bone cement, the setting of CPC-chitosan scaffold takes place at room or body temperature, thereby presenting no risk for the encapsulated cells or the surrounding tissues.[63]

For prophylaxis, it is important that the antibiotic drug release from the CPC-chitosan matrix can reach concentrations above minimum inhibitory concentration (MIC) and avoid sub-inhibitory concentrations for a prolonged duration, which may lead to bacterial resistance.[5] We used the CPCC+5ORZ and CPCC+10ORZ groups for antibacterial experiments, due to the following reasons. First, the degradation of the microbeads would influence the ORZ release and present an extra complicating factor. Second, chitosan has a moderate microbicidal activity. Therefore, we used the CPCC+5ORZ and CPCC+10ORZ groups to keep the content of chitosan consistent with the CPCC group. Then subsequently, the alginate microbeads were used to encapsulate the hPDLSCs. Further study is needed to prepare CPCC+ORZ+hPDLSCbeads construct to be used as the experimental group for antibacterial experiments. And the results revealed that CPCC+10ORZ scaffold exhibited a strong and stable antimicrobial activity against *S. aureus* biofilm. The

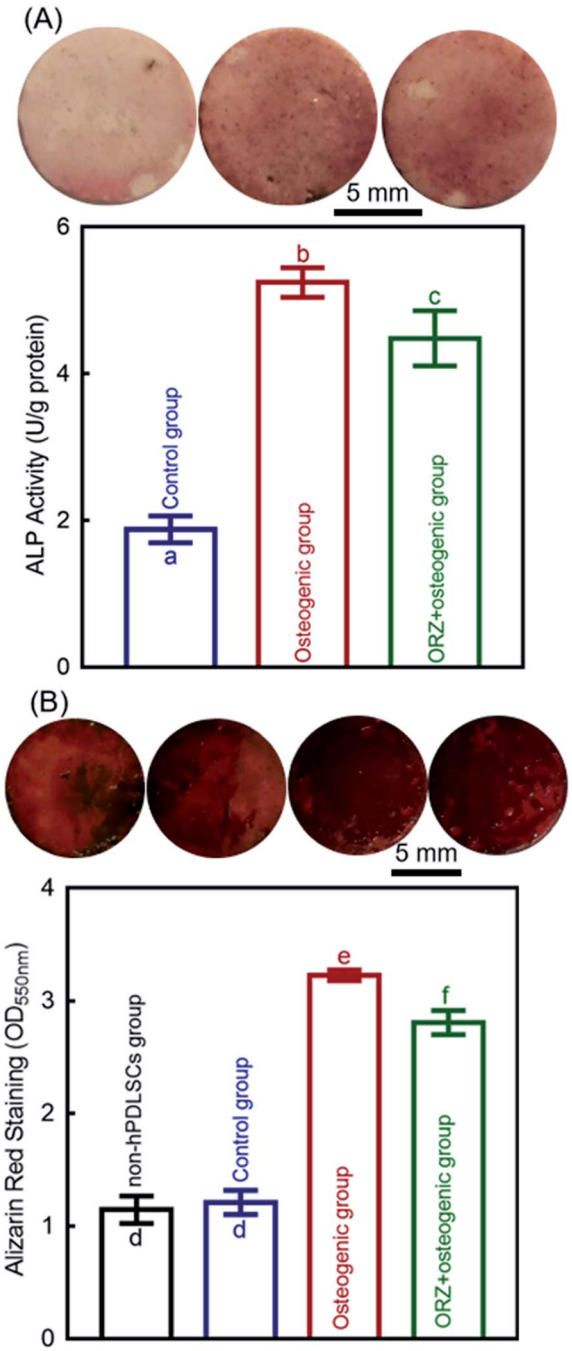

Fig. 9 Osteogenic differentiation of hPDLSCs encapsulated in alginate microbeads in CPC-chitosan scaffolds. (A) Alkaline phosphatase (ALP) staining and quantitative analysis after 14 days of osteogenic induction ($n = 6$). (B) Alizarin Red staining (ARS) and quantitative calculation after 14 days of osteogenic induction ($n = 6$). Dissimilar letters indicate significantly different values ($p < 0.05$).

CPCC+10ORZ scaffold had an initial burst of ORZ release, which was appropriate to have a high local concentration of antibiotic during the initial few hours after the orthopedic surgery to prevent infection.[67,68] Then the scaffold could sustain the ORZ release for up to 6 days, while the released ORZ could be accumulated at the defect site to inhibit bone infections.

The hPDLSCs served as a promising cell source of bone tissue engineering[31,32,42] and showed excellent proliferation on CPC-chitosan scaffolds.[31,42] The alginate microbeads acted as a protection for hPDLSCs during the CPC setting and injection process.[30,63] The CPC control paste exhibited slow setting, especially when porogens and other ingredients were added. However, the addition of chitosan into CPC provided fast-setting and anti-washout capabilities to CPC, due to the high pH of CPC paste causing the chitosan to gel.[69] This reduced the setting time from 69.5 ± 2.1 minutes for CPC control, to only 6.7 ± 1.6 minutes for CPC-chitosan scaffold.[69] In addition, while the CPC control paste showed dissolution during setting in a solution simulating physiological fluid *in vivo*, CPC-chitosan scaffold paste was anti-washout with no dissolution in the solution.[69] Based on these properties, the present study selected CPC-chitosan (CPCC) scaffold for the hPDLSC experiments. In addition, cellular assays including cell viability, proliferation and osteogenic differentiation were performed to investigate the bioactivity of CPCC+10ORZ+hPDLSCbeads. The results showed that the ORZ release did not reduce the cell viability. The attachment and spreading of the cells to the scaffolds confirmed the biocompatibility of the scaffolds. When the culture was prolonged to 14 days, the hPDLSCs were released from the microbeads and successfully synthesized bone minerals. To avoid the interference of minerals in CPC matrix, the ARS staining of non-hPDLSCs group was used as the baseline and subtracted from the measured values with hPDLSCs. And the results revealed that the novel ORZ-loaded scaffold plus osteogenic group had 2.4-fold to 2.3-fold increases in the ALP activity and bone mineral synthesis, compared to control group. These results indicate that the hPDLSCs are promising as a readily-harvestable, autologous and low-cost alternative to the gold-standard hBMSCs. In addition, the novel injectable CPCC+10ORZ+hPDLSCbeads construct is highly promising to deliver both antibiotics and stem cells.

CPC has been used for minimally-invasive applications due to the flowability and injectability of the CPC paste. CPC scaffolds exhibit excellent biocompatibility and osteoconductivity *in vivo* and *in vitro*.[30,31,42,70] Previous studies showed good results in stem cell delivery *via* CPC scaffolds for bone regeneration.[31,42] CPC was implanted into the bone defects in rats, with excellent new bone formation at 12 weeks.[44,70] The new bone contained osteoids with osteocytes, blood vessels, and numerous osteoblasts lining the new bone front.[44,70] Furthermore, compared to CPC scaffold without stem cell delivery, there was much more new bone formation in the groups with CPC delivering cells, including human embryonic stem cells, hiPSCs, hBMSCs, hUCMSCs and hPDLSCs.[31,42,44,70] In addition, CPC could be readily used to deliver drugs and molecules with biological activity, which could be mixed into the CPC paste.[31,42] However, there has been no report on the effects of antibiotic release together with hPDLSC-encapsulating alginate microbeads in CPC. Therefore, the present study was an extension of previous researches,[30,63,71] by combining ORZ and hPDLSCs in an injectable CPC-chitosan scaffold. Compared to the control group, the ORZ-loaded CPC-chitosan-alginate microbead scaffold achieved much greater ALP activity and bone mineral

synthesis by the hPDLSCs. However, ORZ+osteogenic groups had lower osteogenic effect than that without ORZ. A possible reason may be the cellular internalization of ORZ,[20] and the suppression on the cells' activity and protein tyrosine phosphorylation,[72] which are important for cell proliferation and differentiation.[73] This hypothesis needs to be investigated in a further *in vitro* and *in vivo* study.

Various strategies have been explored to regenerate critically-sized bone defects *via* bone tissue engineering, using biomimetic scaffolds and hydrogels for stem cell delivery.[42,74–76] These scaffolds provided novel strategies for stem cell delivery, and they could greatly enhance the osteogenic differentiation and bone mineral synthesis.[42,74–76] Hydrogels could serve as a template for stem cell colonization, proliferation and osteogenic differentiation.[74,75] For example, a synthetic hydrogel–ACP composite increased mineralized extracellular matrix with calcium deposition.[74] In addition, some drugs and molecules with biological activity could be loaded into scaffolds and hydrogels to promote cell vitality and adhesion, including fetal serum, human platelet lysate (hPL), chemotactic growth factors (GFs), *etc.*[31,42,74,75] Furthermore, RGD-CPC with stem cell bi-culture and tri-culture achieved prevascularization to enhance the bone regeneration and blood vessel formation *in vivo*.[76] In addition, metformin- and hPL-loaded hPDLSC-CPC constructs showed that metformin and hPL release from CPC scaffold supported the hPDLSCs and promoted the osteogenic differentiation and bone mineral synthesis.[31,42] Therefore, these scaffolds have the potential to provide a clinical grade of biomedical device. However, the ability of bone formation and absorption time of these bone substitute materials in the body should be investigated.[77] In addition, their usage in dental, craniofacial and orthopedic applications should also evaluated.[77] A previous study on bone augmentation in major oral and maxillofacial surgeries in a preclinical trial showed that the OCP/atelocollagen (Col) construct enhanced bone regeneration in human bone defects.[77] Further study is needed to follow previous studies[77,78] and evaluate the clinical applications of CPC scaffolds.

An ongoing clinical challenge in bone repair is the high possibility of infection, which delays and compromises the healing process. To facilitate clinical applications, it would be desirable to develop a scaffold to deliver antibiotics in bone defects for local release and infection-control. The new injectable antibiotic-loaded and stem cell-encapsulated CPC scaffold is a promising approach to overcome the infection problem in wound healing. The injectable CPCC+10ORZ+hPDLSCbeads construct could be used after orthopedic surgery, or could be injected into the periodontal pockets for the treatment of periodontitis and bone regeneration in clinical applications. Further studies and animal testing are needed to investigate the local anti-infection ability, biofilm-killing potency and bone regeneration efficacy *in vivo* and in clinical trial of this new construct.

5. Conclusion

This study developed a novel injectable ORZ-loaded CPC-chitosan-alginate microbead scaffold and investigated its effects on *S. aureus* infection inhibition and osteogenic differentiation of hPDLSCs. The 10% ORZ incorporation did not affect the mechanical characteristics of the CPC scaffold. With 6 days of sustained ORZ release, the CPCC+10ORZ scaffold had excellent antibacterial function against *S. aureus*, with an inhibition zone of 12 mm and no colony formation. The construct with 50% by volume of microbeads encapsulating hPDLSCs yielded successful cell differentiation into the osteogenic lineage. Furthermore, the ORZ scaffold+osteogenic group had more than 2 folds of increase in ALP activity and bone mineral synthesis, compared to control group. Hence, the ORZ-releasing CPC scaffold has multiple biofunctions with excellent infection-prevention and osteogenesis-promotion capabilities. The novel CPCC+10ORZ+hPDLSCbeads construct is highly promising for dental, craniofacial and orthopedic applications to inhibit infections and enhance bone regeneration.

Conflicts of interest

There are no conflicts to declare.

References

1 J. S. Moskowitz, M. R. Blaisse, R. E. Samuel, H.-P. Hsu, M. B. Harris, S. D. Martin, J. C. Lee, M. Spector and P. T. Hammond, *Biomaterials*, 2010, **31**, 6019–6030.
2 A. Jenkins, B. A. Diep, T. T. Mai, N. H. Vo, P. Warrener, J. Suzich, C. K. Stover and B. R. Sellman, *mBio*, 2015, **6**(1), e02272-14.
3 K. Malizos, J. Sarma, R. Seaton, M. Militz, F. Menichetti, G. Riccio, J. Gaudias, U. Trostmann, R. Pathan and K. Hamed, *Eur. J. Clin. Microbiol. Infect. Dis.*, 2016, **35**, 111–118.
4 S. A. Horst, V. Hoerr, A. Beineke, C. Kreis, L. Tuchscherr, J. Kalinka, S. Lehne, I. Schleicher, G. Köhler and T. Fuchs, *Am. J. Pathol.*, 2012, **181**, 1206–1214.
5 R. Jayasree, T. S. Kumar, G. Perumal and M. Doble, *Ceram. Int.*, 2018, **44**, 9227–9235.
6 W. Reizner, J. Hunter, N. O'Malley, R. Southgate, E. Schwarz and S. Kates, *Eur. Cells Mater.*, 2014, **27**, 196.
7 N. K. Archer, M. J. Mazaitis, J. W. Costerton, J. G. Leid, M. E. Powers and M. E. Shirtliff, *Virulence*, 2011, **2**, 445–459.
8 S. Ranghar, P. Sirohi, P. Verma and V. Agarwal, *Eur. Cells Mater.*, 2014, **57**, 209–222.
9 B. Tuleubaev, D. Saginova, T. Abiyev, M. Davletbaev and A. Koshanova, *Georgian Med. News*, 2016, 21–26.
10 S. K. Nandi, S. Bandyopadhyay, P. Das, I. Samanta, P. Mukherjee, S. Roy and B. Kundu, *Biotechnol. Adv.*, 2016, **34**, 1305–1317.
11 A. Ewald, D. Hösel, S. Patel, L. M. Grover, J. E. Barralet and U. Gbureck, *Acta Biomater.*, 2011, **7**, 4064–4070.
12 E. Vorndran, M. Geffers, A. Ewald, M. Lemm, B. Nies and U. Gbureck, *Acta Biomater.*, 2013, **9**, 9558–9567.
13 D. Pastorino, C. Canal and M.-P. Ginebra, *Acta Biomater.*, 2015, **12**, 250–259.
14 M.-P. Ginebra, C. Canal, M. Espanol, D. Pastorino and E. B. Montufar, *Adv. Drug Delivery Rev.*, 2012, **64**, 1090–1110.

15 L. A. Diaz-Gomez, P. D. Kontoyiannis, A. J. Melchiorri and A. G. Mikos, *Tissue Eng., Part C*, 2019.
16 H. H. Xu, P. Wang, L. Wang, C. Bao, Q. Chen, M. D. Weir, L. C. Chow, L. Zhao, X. Zhou and M. A. Reynolds, *Bone Res.*, 2017, **5**, 17056.
17 Y. Xia, H. Chen, Y. Zhao, F. Zhang, X. Li, L. Wang, M. D. Weir, J. Ma, M. A. Reynolds and N. Gu, *Mater. Sci. Eng., C*, 2019, **98**, 30–41.
18 M. D. Weir and H. H. Xu, *Acta Biomater.*, 2010, **6**, 4118–4126.
19 M. D. Weir, H. H. Xu and C. G. Simon Jr, *J. Biomed. Mater. Res., Part A*, 2006, **77**, 487–496.
20 E. Başaran, B. Şenel, G. Yurtdaş Kırımlıoğlu, U. M. Güven and Y. Yazan, *Lat. Am. J. Pharm.*, 2015, **34**, 1180–1188.
21 L. Casettari, D. Vllasaliu, E. Castagnino, S. Stolnik, S. Howdle and L. Illum, *Prog. Polym. Sci.*, 2012, **37**, 659–685.
22 W. Zimmerli, in *Osteomyelitis. of. the. Jaws*, ed. T. Abiyev, Springer, 2009, pp. 179–190.
23 R. J. Dias, V. D. Havaldar, V. S. Ghorpade, K. K. Mali, V. K. Gaikwad and D. M. Kumbhar, *J. Appl. Pharm. Sci.*, 2016, **6**, 200–209.
24 P. Ravishankar, Y. P. Kumar, E. Anila, P. Chakraborty, M. Malakar and R. Mahalakshmi, *Int. J. Pharm. Invest.*, 2017, **7**, 188.
25 J. D. Caplin and A. s. J. GarcÃ-a, *Acta Biomater.*, 2019, **93**, 2–11.
26 Y. Lu, M. Li, L. Li, S. Wei, X. Hu, X. Wang, G. Shan, Y. Zhang, H. Xia and Q. Yin, *Mater. Sci. Eng., C*, 2018, **82**, 225–233.
27 W. Chen, X. Liu, Q. Chen, C. Bao, L. Zhao, Z. Zhu and H. H. Xu, *J. Tissue Eng. Regener. Med.*, 2018, **12**, 191–203.
28 L. Zhao, M. D. Weir and H. H. Xu, *Biomaterials*, 2010, **31**, 3848–3857.
29 Y. Zhang, Y. Xing, L. Jia, Y. Ji, B. Zhao, Y. Wen and X. Xu, *Stem Cells Dev.*, 2018, **27**, 1634–1645.
30 L. Zhao, M. D. Weir and H. H. Xu, *Biomaterials*, 2010, **31**, 6502–6510.
31 Z. Zhao, J. Liu, M. D. Weir, N. Zhang, L. Zhang, X. Xie, C. Zhang, K. Zhang, Y. Bai and H. H. Xu, *RSC Adv.*, 2019, **9**, 41161–41172.
32 J. Liu, Z. Zhao, J. Ruan, M. D. Weir, T. Ma, K. Ren, A. Schneider, T. W. Oates, A. Li and L. Zhao, *J. Dent.*, 2020, **92**, 103259.
33 I. C. Gay, S. Chen and M. MacDougall, *Orthodontics & Craniofacial Research*, 2007, **10**, 149–160.
34 K. G. Silvério, T. L. Rodrigues, R. D. Coletta, L. Benevides, J. S. Da Silva, M. Z. Casati, E. A. Sallum and F. H. Nociti Jr, *J. Periodontol.*, 2010, **81**, 1207–1215.
35 D. Menicanin, K. M. Mrozik, N. Wada, V. Marino, S. Shi, P. M. Bartold and S. Gronthos, *Stem Cells Dev.*, 2014, **23**, 1001–1011.
36 B.-M. Seo, M. Miura, S. Gronthos, P. M. Bartold, S. Batouli, J. Brahim, M. Young, P. G. Robey, C. Y. Wang and S. Shi, *Lancet*, 2004, **364**, 149–155.
37 K. Y. Lee and D. J. Mooney, *Prog. Polym. Sci.*, 2012, **37**, 106–126.
38 W. R. Gombotz and S. F. Wee, *Adv. Drug Delivery Rev.*, 2012, **64**, 194–205.
39 R. S. Ashton, A. Banerjee, S. Punyani, D. V. Schaffer and R. S. Kane, *Biomaterials*, 2007, **28**, 5518–5525.
40 E. Alsberg, H. Kong, Y. Hirano, M. Smith, A. Albeiruti and D. Mooney, *J. Dent. Res.*, 2003, **82**, 903–908.
41 H. Zhou and H. H. Xu, *Biomaterials*, 2011, **32**, 7503–7513.
42 Z. Zhao, J. Liu, A. Schneider, X. Gao, K. Ren, M. D. Weir, N. Zhang, K. Zhang, L. Zhang and Y. Bai, *J. Dent.*, 2019, **91**, 103220.
43 H. H. Xu, J. B. Quinn, S. Takagi, L. C. Chow and F. C. Eichmiller, *J. Biomed. Mater. Res.*, 2001, **57**, 457–466.
44 W. Chen, J. Liu, N. Manuchehrabadi, M. D. Weir, Z. Zhu and H. H. Xu, *Biomaterials*, 2013, **34**, 9917–9925.
45 J. Liu, W. Chen, Z. Zhao and H. H. Xu, *Acta Biomater.*, 2014, **10**, 5128–5138.
46 J. Liu, W. Chen, Z. Zhao and H. H. Xu, *Biomaterials*, 2013, **34**, 7862–7872.
47 K. Lee, M. D. Weir, E. Lippens, M. Mehta, P. Wang, G. N. Duda, W. S. Kim, D. J. Mooney and H. H. Xu, *Dent. Mater.*, 2014, **30**, e199–e207.
48 E. F. Burguera, H. H. Xu and L. Sun, *J. Biomed. Mater. Res., Part B*, 2008, **84**, 493–502.
49 H. H. Xu, J. B. Quinn, S. Takagi and L. C. Chow, *Biomaterials*, 2004, **25**, 1029–1037.
50 Z. Liu, L. Yuan and J. Yu, *Adv. Appl. Ceram.*, 2019, **118**, 249–256.
51 E. Bruneel, F. Persyn and S. Hoste, *Supercond. Sci. Technol.*, 1998, **11**, 88.
52 L.-C. Wang, X.-G. Chen, D.-Y. Zhong and Q.-C. Xu, *J. Biomed. Mater. Res., Part B*, 2007, **18**, 1125–1133.
53 H. N. Pei, X. G. Chen, Y. Li and H. Y. Zhou, *J. Biomed. Mater. Res., Part A*, 2008, **85**, 566–572.
54 Y. Chang, J. Bai, J.-H. Lee and S. Ryu, *Food Microbiol.*, 2019, **82**, 523–532.
55 L. Wang, X. Xie, S. Imazato, M. D. Weir, M. A. Reynolds and H. H. Xu, *Mater. Sci. Eng., C*, 2016, **67**, 702–710.
56 M. Malwal and R. Sarin, *Indian J. Nat. Prod. Res.*, 2011, **2**, 48–51.
57 X. Lv, Z. Li, S. Chen, M. Xie, J. Huang, X. Peng, R. Yang, H. Wang, Y. Xu and C. Feng, *Biomaterials*, 2016, **84**, 99–110.
58 L. Cheng, M. D. Weir, K. Zhang, D. D. Arola, X. Zhou and H. H. Xu, *J. Dent.*, 2013, **41**, 345–355.
59 H. Chen, B. Zhang, M. D. Weir, N. Homayounfar, G. G. Fay, F. Martinho, L. Lei, Y. Bai, T. Hu and H. H. Xu, *J. Dent.*, 2020, 103278.
60 M. Sandberg, A. Määttänen, J. Peltonen, P. M. Vuorela and A. Fallarero, *Int. J. Antimicrob. Agents*, 2008, **32**, 233–240.
61 H. Wang, S. Wang, L. Cheng, Y. Jiang, M. A. S. Melo, M. D. Weir, T. W. Oates, X. Zhou and H. H. Xu, *Mater. Sci. Eng., C*, 2019, **94**, 587–596.
62 D.-C. Yang, M.-H. Yang, C.-C. Tsai, T.-F. Huang, Y.-H. Chen and S.-C. Hung, *PLoS One*, 2011, **6**(9), e23965.
63 L. Wang, C. Zhang, C. Li, M. D. Weir, P. Wang, M. A. Reynolds, L. Zhao and H. H. Xu, *Mater. Sci. Eng., C*, 2016, **69**, 1125–1136.
64 C. J. Damien and J. R. Parsons, *J. Appl. Biomater.*, 1991, **2**, 187–208.

65 T. A. Russell and G. Insley, *Orthop. Clin. N. Am.*, 2017, **48**, 289–300.
66 R. N. Shamma, N. A. Elkasabgy, A. A. Mahmoud, S. I. Gawdat, M. M. Kataia and M. A. A. Hamid, *Int. J. Pharm.*, 2017, **521**, 306–317.
67 K. Gulati, M. S. Aw and D. Losic, *Nanoscale Res. Lett.*, 2011, **6**, 1–6.
68 H. Winkler and P. Haiden, *Operative Techniques in Orthopaedics*, 2016, **26**, 2–11.
69 H. H. Xu, S. Takagi, J. B. Quinn and L. C. Chow, *J. Biomed. Mater. Res.*, 2004, **68**, 725–734.
70 P. Wang, X. Liu, L. Zhao, M. D. Weir, J. Sun, W. Chen, Y. Man and H. H. Xu, *Acta Biomater.*, 2015, **18**, 236–248.
71 H. Zhou, W. Chen, M. D. Weir and H. H. Xu, *Tissue Eng., Part A*, 2012, **18**, 1583–1595.
72 A. B. Siva, C.-H. Yeung, T. G. Cooper and S. Shivaji, *Reprod. Toxicol.*, 2006, **22**, 702–709.
73 Y. Ren, L. Yu, J. Fan, Z. Rui, Z. Hua, Z. Zhang, N. Zhang and G. Yin, *Mol. Cell. Biochem.*, 2012, **365**, 109–118.
74 A. S. Chahal, M. Schweikle, A.-M. Lian, J. E. Reseland, H. J. Haugen and H. Tiainen, *J. Tissue Eng.*, 2020, **11**, 2041731420926840.
75 F. Re, L. Sartore, V. Moulisova, M. Cantini, C. Almici, A. Bianchetti, C. Chinello, K. Dey, S. Agnelli and C. Manferdini, *J. Tissue Eng.*, 2019, **10**, 2041731419845852.
76 Y. Lin, S. Huang, R. Zou, X. Gao, J. Ruan, M. D. Weir, M. A. Reynolds, W. Qin, X. Chang and H. Fu, *Dent. Mater.*, 2019, **35**, 1031–1041.
77 T. Kawai, S. Kamakura, K. Matsui, M. Fukuda, H. Takano, M. Iino, S. Ishikawa, H. Kawana, T. Soma and E. Imamura, *J. Tissue Eng.*, 2020, **11**, 2041731419896449.
78 T. Kawai, S. Echigo, K. Matsui, Y. Tanuma, T. Takahashi, O. Suzuki and S. Kamakura, *Tissue Eng., Part A*, 2014, **20**, 1336–1341.